Percolation scaling, inhomogeneity, and defects in polyaniline blends: A $1/f$ noise diagnosis

Jérôme Planès* and Arnaud François
Laboratoire de Physique des Métaux Synthétiques, UMR 5819 CEA-CNRS-Université Joseph Fourier, Département de Recherche Fondamentale sur la Matière Condensée, CEA-Grenoble, 17 rue des Martyrs, F-38054, Grenoble, Cedex 9, France
(Received 16 January 2004; revised manuscript received 6 August 2004; published 8 November 2004)

The resistance fluctuation properties of a family of conducting polymer blends, poly(aniline)/poly(methyl methacrylate), are investigated as a function of conducting phase mass fraction. The blends exhibit $1/f$ noise according to Hooge's empirical formula. The noise amplitude scales with the conducting phase mass fraction and the resistance as expected by the percolation theory. The exponents of the scaling laws are within the bounds of the extended random void model, derived in the continuous percolation scheme. Noise characterization proves to be a much more sensitive tool to local current heterogeneities than resistance. As a consequence, sample preparation, sample holder design, and absence of defects are prominent criteria for convenient noise amplitude estimation. Surface effects, contact noise, and influence of geometrical defects are studied and analyzed.

DOI: 10.1103/PhysRevB.70.184203 PACS number(s): 72.70.+m, 72.20.−i, 73.61.Ph, 68.35.Dv

I. INTRODUCTION

Transport properties of organic conducting blends made of doped conducting polymer poly(aniline) (PANI) and some conventional insulating matrix have attracted much interest because of the percolative nature at very low critical mass fraction p_c of the conductive phase: 0.1% or even less. This was first demonstrated more than ten years ago[1] with matrix poly(methyl methacrylate) (PMMA), using cosolution processing in solvent *m*-cresol. Numerous experimental techniques have been used to investigate this complex system including electronic properties (dc and ac resistivity at variable temperature, magnetoresistance, electron spin resonance, etc.),[2,3], microstructure (by transmission electron microscopy or atomic force microscopy),[4,5] and mechanical properties.[6]

The key parameter governing transport in conducting polymers is disorder. It is found at many length scales and is due to conjugation defects, ends of finite length polymer chains, uneven repartition of dopants, and partial crystallinity. The latter creates microstructural inhomogeneities which are thought to be responsible for, or at least correlated to, electronic inhomogeneities.[7] In the case of PANI doped with campor sulfonic acid (CSA), this picture of the material gives a model for the nonmonotonic behavior of the thermal dependence of resistivity, which would be difficult to understand in the homogeneous view of Mott-Anderson disorder.[8] The same behavior is observed when PANI(CSA) is blended with PMMA.

As a consequence of disorder and heterogeneity, these conductors are expected to exhibit low-frequency excess noise, of $1/f$ noise. Moreover, percolation theories predict that the noise amplitude $\mathcal{S}$ is also a diverging quantity as the conductive phase fraction p approaches the percolation threshold from above:

$$\mathcal{S} \propto (p - p_c)^{-\kappa}. \tag{1}$$

However, noise investigations in PANI blends cannot be found in the literature, except for a system of PANI particles ($\varnothing \sim 100$ nm) dispersed in poly(vinyl alcohol) which does not percolate even for the largest studied PANI content: 25.7 vol. % (Ref. 9).

We have thus performed a series of noise measurements on the same kind of PANI(CSA)/PMMA films considered in previous transport studies[10,11] in order to get further insight into the conducting processes of this system. Measurements consist of the power spectral density (PSD) of noise—i.e., the repartion of noise power in the frequency domain. Spectra are found to follow Hooge's empirical formula[12]

$$S_V = \alpha_H \frac{V^2}{N_c f}, \tag{2}$$

where V is the voltage difference measured on the sample, N_c the number of carriers,[13] f the frequency, and α_H a numerical value (Hooge's parameter). Therefore the signal for a given sample is entirely determined by the value of S_V/V^2 at a given frequency (1 kHz for the plots in the remainder of the paper.) This value is rigorously identical to S_1/I^2 or S_R/R^2 if the current or the resistance were measured instead of the voltage.

We clearly observe that the noise amplitude follows the scaling law of Eq. (1); however, it has been necessary to carefully analyze the various contributions to noise, as will be thoroughly detailled in the paper, to get reliable exponents. The value $\kappa = 2.19$ seems to confirm that standard lattice percolation[14] is not well suited to describe transport in PANI(CSA)/PMMA blends; this was first suggested by the study of dc resistivity $\rho(p,T)$ as a function of p and temperature.[10,11]. Data were compatible with the extended random void model[15] (see Sec. VI A for a description) which belongs to the class of continuous percolation.[16] In the latter, percolation exponents differ from those of lattice percolation because elementary resistors have a wide diverging distribution of resistances.

The paper is organized as follows. Section II reports on the experimental details of specimen preparation and noise measurements. In Sec. III, the percolative behavior of the

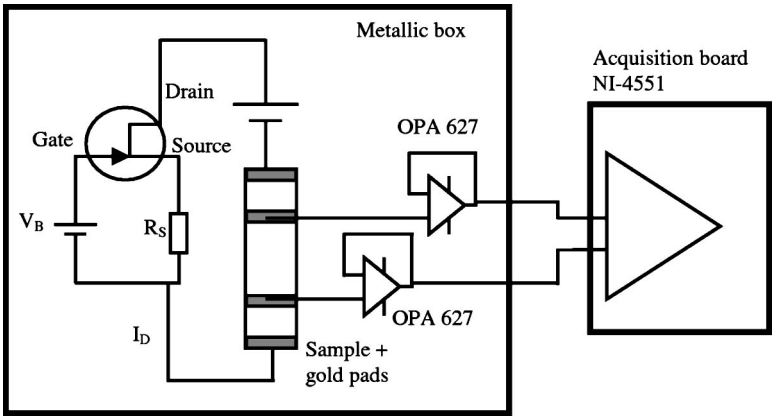

FIG. 1. Block diagram of the experimental setup designed for this study. The transistor used for the low-noise-current source is JFET (2N 54 57). Two low-noise amplifiers OPA 627, powered by batteries, are inserted in the detection chain in order to increase the effective input impedance of the acquisition board.

noise amplitude is described and the exponents given. Those results were obtained after modifications made to the initial sample holder design, in order to get rid of contact noise. This effect leads to interesting information about sample surfaces, which is presented in Sec. IV. It was also necessary to eliminate some "defected" samples in the series. In order to justify the meaning of such a selection, intentional defects were introduced in, then erased from, several samples whose average resistance and resistance fluctuations (noise) were subsequently measured. The procedure, results, and a simple numerical simulation corroborating the analysis are explained in Sec. V. In Sec. VI, we discuss experimental results of the literature concerning conducting blends and showing a wide dispersion, before concluding.

II. EXPERIMENT

Polymer film. The preparation of the composite films used throughout this study has been reported in detail in Ref. 17. Highlights are as follows. Poly(emeraldine) base is mixed with the protonating agent: camphor sulphonic acid (CSA), at 0.5 molar ratio of dopant molecule to PANI mer. From the suspension of this mixture in *m*-cresol at 0.5 wt % PANI content, the so-called soluble part (after centrifugation) is extracted and its concentration determined. This solution is mixed in various ratios with a 5 wt % *m*-cresol solution of PMMA. Solutions are subsequently cast onto a glass plate and the solvant slowly evaporated at temperatures of 50–60 °C, yielding highly flexible and transparent films. Their thickness ranges from 20 to 80 μm.

Measurement setup. Voltage fluctuations are measured while current is kept constant. The most severe constraint in designing the instrumental setup is the wide range of sample impedances: from 100 Ω to 10 MΩ. The block diagram of the setup is drawn in Fig. 1. Traditionnal current sources used for resistance measurements are too noisy for this experiment. A low-noise-current source was built with a junction field-effect transistor JFET (2N 54 57).[18] The signal is digitized and Fourier transformed by NI4551 board (National Instruments). The maximum sampling rate of the board is 204 ksample/s; thus the frequency range for analysis is 10 Hz–95 kHz. The input impedance of the board is 1 MΩ, which is not large enough for our purpose. On each voltage line, a low-noise amplifier OPA 627 is inserted before entry in order to increase the apparent impedance of the detection device. Amplifiers are powered by batteries. The whole setup is inserted as compactly as possible in a metallic box for electromagnetic shielding purpose. Once short-circuited, the instrumental background (white) noise of the setup is 7×10^{-17} V^2 Hz^{-1}.

Sample holder and sample shape. Films are punched so that samples all have the same lateral dimensions. The contact between polymer film and electrodes is traditionally realized by mechanical pressure and without conducting paste because the solvent of the paste could locally interact with the polymer and more specifically modify the doping. In order to minimize the contact resistance, 100-nm-thick gold pads are evaporated onto one side of the films and the electrodes (generally gold wires) are pressed into contact on the pads. Moreover, a four-probe design and the high impedance of the voltmeter prevent current to flow through the contact resistances. This method, extensively used in our previous transport studies, was naturally extrapolated for voltage noise measurements. As will be explained in Sec. IV A, it reveals highly unsatisfactory, because such contacts, being in the current path, act as noise sources, even if no current is derived in the voltage measurement line. For this reason, we had to design a specific sample holder, for which current injection electrodes and voltage probes are not aligned. Therefore, samples are cut in π shape (see Fig. 10). Gold pads for voltage probes lie on π "legs"—i.e., out of the main current path. The "legs" nevertheless contribute to noise, because of their resistance, through thermal noise $4kTR_{\text{legs}}$. This resistance should be minimized by proper legs dimensions. Length is 1.5 mm, width is 1 mm, and they are 4 mm apart. Electrodes are now four independent tips, each of them equiped with a spring.

III. PERCOLATION SCALING

The results reported in this section are obtained with defectless π-shaped samples, for which noise level is reliably thought to come from bulk resistance and not from contacts or isolated defects.

In Fig. 2, the percolation threshold and the resistivity exponent of percolation t are determined by the linear fit of $\ln \rho$ vs $\ln(p-p_c)$, according to the scaling law

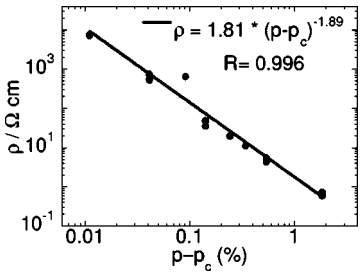

FIG. 2. Log-log plot of resitivity as a function of PANI mass fraction p. Here $p_c=0.16\%$ is the critical fraction or percolation threshold, determined by optimization of the linear alignment. The slope $-t=-1.89$ gives the so-called resistivity exponent of percolation.

$$\rho \propto (p - p_c)^{-t}. \tag{3}$$

$t=1.89$ at room temperature is close to what was found previously.[11] The critical mass fraction is found to be $p_c=0.16\%$.

The same value for p_c is used in Fig. 3 to plot the relative noise amplitude S_V/V^2 at 1 kHz vs $p-p_c$ in a double-logarithmic representation. The noise exponent is $\kappa=2.19$.

The scaling of ρ and S_V/V^2 (or identically S_ρ/ρ^2) with the same variable $p-p_c$ induces

$$S_V/V^2 \propto \rho^w. \tag{4}$$

For our data, it is shown in Fig. 4, with $w=1.16$. Obviously Eq. (4) does not contain supplementary information once percolation scaling has been checked. However, one of its practical interest is that the uncertainties in experimental quantity p are avoided. In our case it can be seen that the samples corresponding to $p=0.25\%$ ($\rho\sim10^3\ \Omega$ cm and $S_V=1-2\times10^{-14}\ \mathrm{V^2\,Hz^{-1}}$) are not so well aligned in Figs. 2 and 3 as compared to other points. In Fig. 4, conversely, they do collapse with the points corresponding to lower p. It is probably the signature of a surestimated value of p. Similarly, sample-to-sample variations observed in $\rho(p)$ and $S_V(p)$ are partially due to slight differences in actual p values. That is probably why the $S_V(\rho)$ plot and w value are more often found in the literature than the $S_V(p)$ and κ exponent. Nevertheless, it seems important to us to show how far the fit for κ is acceptable. This will be again discussed with respect to published results in Sec. VI B. Comparison of our exponents with those of the literature, experimental and theoretical, will be done in Sec. VI after a detailed report of measurement conditions and artifacts.

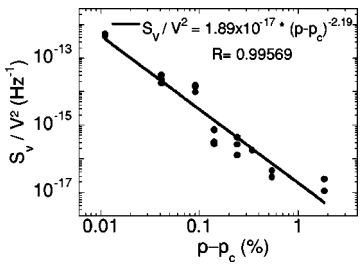

FIG. 3. Log-log plot of relative noise amplitude S_V/V^2 at 1 kHz as a function of PANI mass fraction p. Here $p_c=0.16\%$ as in Fig. 2. The slope $-\kappa=-2.19$ gives the so-called noise exponent of percolation.

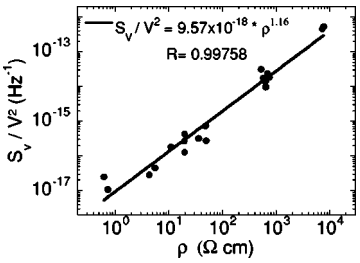

FIG. 4. Scaling of relative noise amplitude S_V/V^2 at 1 kHz vs resistivity ρ. The slope of the fitting curve gives exponent $w=1.16=\kappa/t$.

IV. CONTACT NOISE

In this section, all the experimental data come from measurements made on rectangular samples with voltage probes in the current path, as depicted in Fig. 1.

A. Influence of film side

Whatever the measurement configuration, the PSD of any sample looks like those in Fig. 5. The frequency dependance follows $S_V(f)\propto f^{-\alpha}$ with $\alpha=1.0\pm0.1$. Here α does not depend either on p or on the applied bias voltage. The quadratic dependance of S_V at 1 kHz is shown in Fig. 6 for four different values of p. On average over the ten p values it is found $S_V(V)\propto V^\beta$ with $\beta=1.9\pm0.2$. Noise thus correspond to resistance noise and can be characterized by the relative value S_V/V^2 at a given frequency. This is plotted as a function of $p-p_c$ in Fig. 7. In this figure, data have been divided into two groups, with very different behavior. For example, at $p-p_c=0.6\%$, S_V/V^2 can be 10^{-17} or $10^{-13}\ \mathrm{Hz^{-1}}$. Each group corresponds to films on which gold pads have been evaporated on the same side, with respect to the solvent evaporation process. The "down" side (▼) was in contact with the glass plate; the "up" side (△) was the free surface by which the solvent evaporates into ambient atmosphere. It should be noted that the resistivity value of "up" and "down"

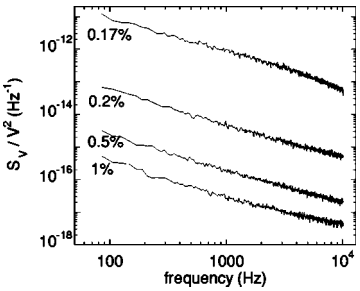

FIG. 5. Power spectral density of noise as a function of frequency for four samples with decreasing PANI content p: 1%, 0.5%, 0.2%, 0.17% from bottom to top. The frequency dependence is $S_V(f)\propto f^{-\alpha}$ with $\alpha=1.0\pm0.1$ on average over ten p values.

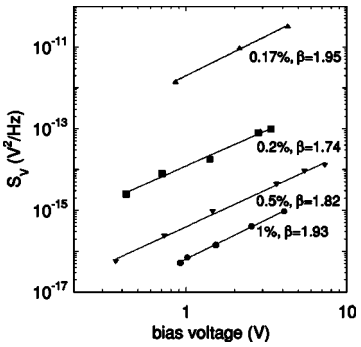

FIG. 6. Noise amplitude at 1 kHz as a function of bias voltage for four samples with decreasing PANI content p: 1%, 0.5%, 0.2%, 0.17% from bottom to top. The bias voltage dependence is $S_V(V) \propto V^{\beta}$ with $\beta = 1.9 \pm 0.2$ on average over ten p values.

samples are identical and that none of the PSD deviates from the general rules recalled above.

The absolute noise amplitude is thus the only feature that distinguishes the two sides. We therefore conclude that a $1/f$ noise source is present at the upper surface (at least) of most of the films.

Contact resistance R_c is reexamined by comparison of two- and four-probe resistivity measurements. It is found that for "down" samples, R_c is at most 10% of the sample resistance, whereas this ratio varies between 20% and 60% for "up" samples. This observation is no longer true at very low p values, for which R_c may be even larger for "down" than for "up" samples. This seems strongly correlated to the behavior or $S_V(p)$ in Fig. 7, where the distinction between sides vanishes as $p \to p_c$.

The comparison between two- and four-probe configuration is subsequently performed for noise measurement. The bias voltage dependence of S_V of sample $p = 0.2\%$ is shown in Fig. 8 for "up" and "down" sides in two- and four-probe configurations. Excess noise observed with two probes on the "up" side exhibits a $1/f$ frequency dependence and V^2 bias voltage dependence. By flowing through contacts, the current clearly reveals $1/f$ resistance noise sources.

B. Interpretation and suppression of contact noise

Our interpretation of former observations is as follows. Gold pads act as equipotentials at the surface. Because their

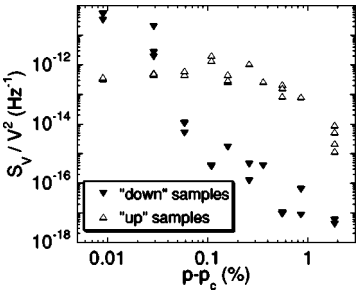

FIG. 7. Same as Fig. 3 for the rectangular samples. The two different symbols correspond to samples for which gold pads have been evaporated on different side, with respect to the solvent evaporation process. For a single p value, S_V/V^2 may change by a factor 10^4 between two samples whose resistance is identical.

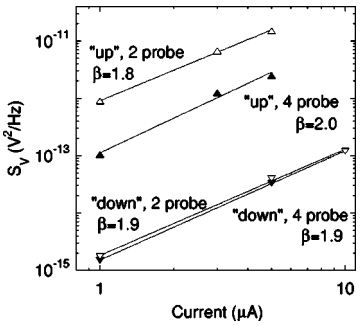

FIG. 8. Noise amplitude, at 1 kHz, in two- and four-probe configurations for "up" and "down" sides of the $p = 0.2\%$ sample. The bias is expressed as a current because this quantity does not depend on R_c values, contrary to the voltage, in the two-probe case.

width is large as compared to the film thickness (1 mm vs 20 μm ca.), the stream lines, parallel to film plane far from the pads, are strongly modified below the pads. The polymer is (at least partially) short-circuited by gold.

The amount of noise generated by the gold-polymer interface naturally depends on the nature of the contact. The two sides of a film are not expected to be equivalent for PANI concentration. The comparison of longitudinal and transverse resistivity measurements shows slight difference, which excludes the presence of any "insulating" or depletion layer. Nevertheless, AFM observations made on surface and cross sections show that the nature of PANI clusters is not identical in both cases.[5] It has also been checked recently that x-ray photoemission spectroscopy (XPS) spectra differ from one side to the other[19]: the absorption edges of N (specific of PANI) and S (specific of the dopant CSA) are only visible for the "down" side. The nature of the very surface of the blend is more favourable to good electrical contacts for the side formerly in contact with glass. At the moment, there are no thermodynamical bases that could justify this difference. Studies about surface tension of doped PANI are few,[20,21] and the results are not easy to ascertain because water easily adsorbs on PANI particles.

Due to the gold shunt of stream lines, correlation methods are not efficient to suppress contact noise. We performed the experiment with a six-probe configuration. The two external electrodes are still used for the current injection and four internal electrodes for the voltage probe. If one indexes probes 1–4, the correlation method consists in measuring the cross correlation between $V_1 - V_3$ and $V_2 - V_4$ instead of the autocorrelation of $V_1 - V_2$ in the standard case. The only common part investigated by carriers is the sample section between probes 2 and 3. None of the wires, connectors, or amplifiers are common to both measures, and therefore their own noise, if any, vanishes in the cross correlation. As a matter of fact, for a sample exhibiting low noise and a vanishingly small contribution of contact noise, the correlation noise may reveal even lower. But contact noise is not suppressed by this method, because the V_2-sample and V_3-sample interfaces are both part of the carrier common path. This is additional evidence for the shunt effect of gold pads.

It seems thus of primary importance for the voltage probe not to disturb stream lines. Reducing the contact area is not

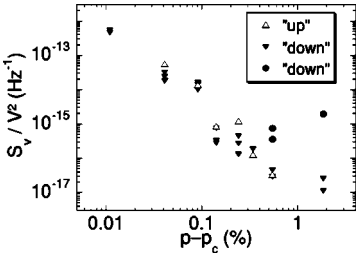

FIG. 9. Log-log plot of relative noise amplitude S_V/V^2 at 1 kHz as a function of PANI mass fraction p as Fig. 3. "Up" and "down" samples are drawn with different symbols, but they no longer differ. Samples represented by ○ are of the "down" group but exhibit anomalously large noise amplitude and are considered as defected ones, as explained in Sec. V.

the solution because the contact resistance will increase subsequently. Therefore we chose to keep a "macroscopic" contact area, aside from main stream lines, whence the π-shape design described in Sec. II.

An alternative geometry has already been used for noise measurement of polymer films.[22] In this work, the sample is electropolymerized on an electrode designed as a Wheatstone bridge. This efficient method would be much more difficult to realize by cutting a self-standing film.

In the recent literature, contact noise suppression is still identified as a complex problem, not readily solved by the four-probe voltage measurement.[23] It was, however, pointed out a long time ago[24] that nonuniform (or "mutispot") contacts yield a noise amplitude strongly dependent on size and density of the "spots." And our case is still more complicated and heterogeneous than the small metallic disks in contact with a uniform semiconductor considered in Ref. 24.

The raw results for the series of π samples are shown in Fig. 9. These are the data used for the determination of exponent κ (Fig. 3). The symbols have the same meaning as for rectangular samples. But there are no more reasons to distinguish them. The same experiment as that depicted by Fig. 8 shows three collapsed curves and only one with a much larger noise level ($\times 10^3$) corresponding to the two-probe configuration for the "up" sample (△).

Three points (○) are put apart in Fig. 9. Despite their being π shaped and belonging to the "down" group, these samples exhibit an anomalously large value of S_V. In percolation theory, it is known that the sample-to-sample variation is a characteristic feature of the proximity to threshold. Our observation is obviously not related to this effect, since it occurs for the most conducting samples—i.e., far from the threshold and for the less noisy samples, in principle.

The explanation of this observation is the subject of the next section and relies on the idea that π samples are subjected to geometrical defects (accidental knife cuts) during preparation.

V. INFLUENCE OF DEFECTS

For the purpose of electrical noise phenomena, the notion of a defect represents any unexpected source of excess noise, which tends to mask the bulk noise, by virtue of the magnifying effect of the fluctuation measurement. As seen before, noise generated by such an isolated source has all the characteristics of "good $1/f$ noise" but its large magnitude reflects its extrinsic nature. On a resistor network, this will happen if somewhere the local current becomes much higher than its average value, what is called current crowding.[25] The proximity of some macroscopic insulating area will promote current crowding.

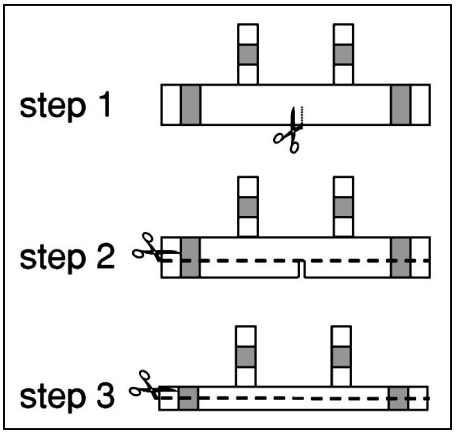

FIG. 10. The three steps of the "experimental simulation" of the effect of intentional defect on resistance and noise. Step 1: the clean sample is cut perpendicularly to the streamlines over roughly half its width, on the opposite side of thevoltage probe (the π legs). Step 2: the damaged sample is cut in order to "erase" the defect—i.e. parallel to the stream lines; the remaining part is thus identical to the initial sample, except that its section is halved. Step 3: similar to step 2, leaving in priciple a clean sample, with a smaller section. Grey areas depict gold pads.

Close to the percolation threshold, the above description loses its simplicity, because heterogeneity is strong and the distribution of local currents naturally wide. That is confirmed in the two next paragraphs reporting the "simulations" of a damage in a previously clean sample and comparing the noise level. These are physical (Sec. V A) and numerical (Sec. V B) experiments.

A. Experimental simulation of intentional defects

Six samples (two for each p value: 0.7%, 0.4%, and 0.2%) have been tested according to the procedure depicted in Fig. 10. The initial samples were chosen such that their noise level correspond to the expectation in agreement with the $S_V(p)$ curve. At each step, it was checked that the PSD follows $S_V \propto V^2/f$. Consequently the results are presented in Fig. 11 as S_V/V^2 as a function of R.

One can see that the scenario is qualitatively identical for each sample. After step 1 (the knife cut), resistance slightly increases by ca. 30%, whereas noise increases dramatically. Quantitatively it is seen that the less resistive the sample, the stronger the noise is enhanced. After step 2 (defect erasure), resistance approximately doubles with respect to its initial value, which is expected because this section is approximately halved, and so does noise, which is also expected because the volume is also halved. The noise source introduced by the cut disappears in the fixed sample. After step 3

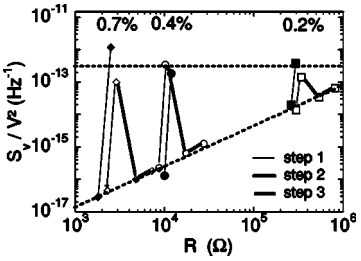

FIG. 11. Relative noise amplitude at 1 kHz vs resistance for two samples of each PANI content $p=0.7\%$ ($\diamond$), $p=0.4\%$ ($\bigcirc$), and $p=0.2\%$ ($\square$). The steps of the scenario described in Fig. 10 are represented by solid lines joining identical symbols. Dashed lines join symbols representing clean (bottom line) and damaged (top line) samples; the $S_V(R)$ dependences dramatically differ.

(proper section reduction), the evolution of R and S_V remains standard.

Two dashed lined are drawn in Fig. 11. They join symbols representing clean (i.e., in the initial state or after step 2) and damaged (i.e. after step 1) samples, respectively. They roughly describe two very different $S_V(R)$ relationships. The horizontal line (top) means that R and S_V are no longer correlated in the presence of a dominating noise source, even if it is still true resistance noise. For some samples a second and a third cut more or less parallel to the first one have been added. There is no significant modification of the noise amplitude, as if a maximum perturbation was reached by a single cut, and a single crack tip was a hottest spot for noise. The bottom dashed line has no physical ground, because the $S_V(R)$ relationships due to a change in p or a change in the sample volume are not identical. Moreover, sample sizes may differ and, thus, resistances are not directly comparable. Nevertheless, in strong contrast with the top line, this pseudocorrelation indicates that the sources for resistance and for noise are of the same nature—i.e., that the whole bulk is concerned.

This experimental simulation shows how one can find two samples with overall identical electrical characteristics (resistance, ohmicity, exhibiting $1/f$ resitance noise) but a completely different noise level. That reveals some specific feature of the specimen, not representative of the bulk. The discussion of Sec. IV can be integrated in this view, considering that the very surface of the film, exposed to air during the drying process, contains localized defects at the interface with gold pads electrodes: a very low surfacic density of contacts between PANI and gold.

All these effects have been extensively used in inorganic semiconductors, using noise as a diagnostic tool for quality and reliability of electronic devices.[26]

B. Numerical simulation of intentional defects

Our interpretation of the results of the previous experiment roughly considers a simplified image in which one can distinguish between "regularly heterogeneous" and "defected" samples. As mentionned at the beginning of Sec. V, the proximity to percolation threshold makes this distinction less accurate. In a resistor network close to p_c, the probability of red bonds, supporting all the current, increases. There is no means of discriminating the effect of a red bond and that of any intentional defect introduced in a regular sample. That is why, at sufficiently low p, the noise level is hardly modified by an extrinsic cause, conversely to larger p where such an intentional defect introduces high current values deep in the tail of the local current distribution.

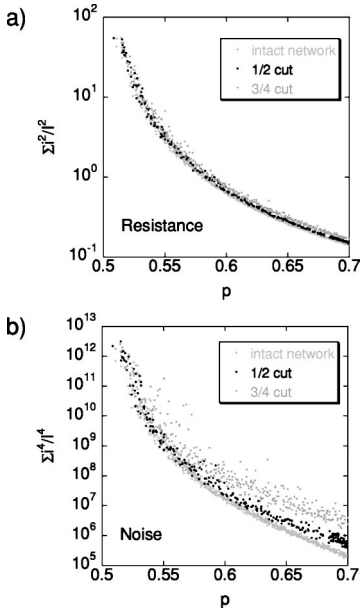

FIG. 12. Dependence of the second (a) and fourth (b) moment of the current distribution on a 2D square random resitor lattice on the fraction of conducting bond. A clean and two damaged series are compared. The defects are made by removing resistors midway from electrodes on, respectively, $1/2$ and $3/4$ of the sample width.

Using the ability, in random resistor networks, to express macroscopic resistance and noise as a function of momenta of current distributions (see Sec. VI A) we explore the above-mentioned effect by numerical simulation. This is done in a very crude way, with the simplest configuration: a square lattice with 1024 bonds between electrodes and 128 bonds plus periodic boundary conditions in the perpendicular direction. Each bond is occupied with probability p by a resistor of resistance unity and empty (insulating) with probability $1-p$. Each resistor has a $1/f$ PSD of noise.

We solve Kirchhoff equations at each node, yielding to the local potential ($\Delta V=1$ between bar electrodes) and then to the local current I_α on each bond α of the backbone (dead ends do not carry current). The total current I is of course dependent on p. The quantity of interest is thus the distribution of relative local currents $i_\alpha=I_\alpha/I$ from which are computed the second moment $M_2=\Sigma_\alpha i_\alpha^2$ proportional to resistance R and the fourth one $M_4=\Sigma_\alpha i_\alpha^4$, proportional to the noise amplitude S_R.

We have performed the calculation for 400 networks with p ranging from 0.5 [$=p_c$ for the two-dimensional (2D) square lattice] to 0.7. It is renewed for different types of damaged lattice. The comparison is shown in Fig. 12 for one clean and two damaged series. The damage consists in removing consecutive resistors, parallel to the main stream, midway from the two bar electrodes. The number of removed resistors cor-

TABLE I. Theoretical values of percolation exponents of resistivity and noise for various models: discrete lattice, discrete lattice with dynamical disorder, random void (RV) and its extended version, inverted random void (IRV) and its extended version, and tunneling percolation (TP).

	2D			3D		
Model	t	κ	w	t	κ	w
Lattice	1.29	1.12	0.87	2.0	1.56	0.78
Disord. latt.	t_{latt}^{2D}	3.1	2.6			
RV	t_{latt}^{2D}	4.10	3.16	2.5	5.05	2.02
Ext. RV	$t_{\text{latt}}^{2D}\to\infty$	$\kappa_{\text{latt}}^{2D}\to\infty$	0.87−4.7	$t_{\text{latt}}^{3D}\to\infty$	$\kappa_{\text{latt}}^{3D}\to\infty$	0.78−2.1
IRV	t_{latt}^{2D}	$\kappa_{\text{latt}}^{2D}$	w_{latt}^{2D}	t_{latt}^{3D}	4.58	2.29
Ext. IRV	t_{latt}^{2D}	$\kappa_{\text{latt}}^{2D}$	w_{latt}^{2D}	$t_{\text{latt}}^{3D}\to\infty$	$\kappa_{\text{latt}}^{3D}\to\infty$	0.78−3.0
TP				$t_{\text{latt}}^{3D}+\lambda/\chi-1$	$\kappa_{\text{latt}}^{3D}+1$	$2.56(\lambda/\chi+1)^{-1}$

responds to 1/2 and 3/4 of the sample width, respectively.

It is seen in Fig. 12 that the behaviors of M_2 and M_4 with respect to the introduction of defects are significantly different. Changes in M_2 are hardly seen, and there is no evidence for the spreading of resistance values. Conversely, M_4 values are increased and spread. The effect is stronger for the more severe 3/4 cut than for the 1/2 cut, and the difference between the three series is emphasized for the largest p, but blurred close to p_c.

Due to the small size of the simulations, they are not free of finite-size effects. Looking at the resistivity exponent of percolation, the best fit is $t=1.2$ instead of $t_{\text{latt}}^{2D}=1.3$. Similarly the noise exponent extracted from the slope $2+w$ in a double-logarithmic plot of M_4 vs M_2 is $w=0.75$ instead of $w_{\text{latt}}^{2D}=0.87$.

By this simulation, we again confirm that it is possible to "build" two systems very close to each other (same p), whose average resistances coincide but resistance fluctuations strongly differ. It was not intended to mimic our materials, which we suppose to contain a wide diverging distribution of local resistances. Nevertheless, the above observation on a simple binary system is expected to remain valid in the more complicated experimental case.

Let us finally note that we assume in this calculation that all resistors remain Ohmic whatever the local current. Considering nonlinearity at high field could be a natural extension.

VI. GENERAL DISCUSSION AND CONCLUSION

A. Theoretical predictions of percolation

The above analysis of "defect noise" in Sec. V B is based on percolation theory. $1/f$ noise in a percolating network was first investigated by Rammal *et al.*[27] The $1/f$ spectral density is not the result of percolation; it is assumed to be present at the scale of the elementary resistors. The specific feature of the critical behavior is the relationship between the noise amplitude $\mathcal{S}$ and fraction of conducting bonds p [Eq. (1)].

The exponent κ is not related to the exponent β that describes the number of bonds participating in the infinite cluster, the one that carries current through the sample. A much smaller part of the bonds determines the noise of the entire lattice, and therefore $\kappa>\beta$.

On a discrete lattice where elementary resistors r_α are subjected to uncorrelated fluctuations δr_α, Cohn's theorem states that the fluctuation of the macroscopic resistance R is

$$\delta R=\sum_\alpha \delta r_\alpha i_\alpha^2. \tag{5}$$

Resistance itself is given by

$$R=\sum_\alpha r_\alpha i_\alpha^2, \tag{6}$$

expressing the identity of the total Joule power and the sum of Joule powers dissipated in the r_α's.

As a consequence,

$$\tilde{S}(f)=\frac{2\langle\delta R^2\rangle_\omega}{R^2}=\frac{2\sum_{\alpha\beta}\delta r_\alpha\delta r_\beta i_\alpha^2 i_\beta^2}{(\sum_\alpha r_\alpha i_\alpha^2)^2}. \tag{7}$$

In the case of identical resistors, elementary fluctuations verify

$$\tilde{s}(f)=\frac{2\langle\delta r^2\rangle_\omega}{r^2}, \tag{8}$$

and thus

$$\tilde{S}(f)=\tilde{s}(f)\frac{\sum_\alpha i_\alpha^4}{(\sum_\alpha i_\alpha^2)^2}, \tag{9}$$

the dependence with the conducting fraction p being realized by the second term on the right-hand side of Eq. (9).

The exponent κ has been computed[27,28] for a binary system on a square or cubic lattice (see Table I). In 2D, the effect of a dynamical disorder has been shown[29] to modify the noise exponents, not the resistance exponent, as expected. In this work, excess disorder is introduced by the competition of the breaking and recovering of elementary resistors, which yield to a stationary state for convenient choices of the probabilities of both events.

TABLE II. Experimental noise exponents in 3D composites. CB is carbon black.

Composites	Exponents	References
CB/Wax	$t=2.3$, $\kappa=4.0$, $w=1.7$	Chen and Chou[a]
AgPt/Tetrafluoroethylene	$w=1$ far from p_c	Rudman *et al.*[b]
	$w=3$ close to p_c	
CB/wax	$t=2.1$, $\kappa=3.6$, $w=1.7$	Nandi *et al.*[c]
Graphite/boron nitride	$w=1.47$ ∥ to compression	Wu and McLachlan[d]
	$w=1.72$ ⊥ to compression	
CB/polyesterimide	$w=1.12$ for high structure CB[e]	Dziedzic and Kolek[f]
	$w=0.76$ for low structure CB	
CB/polymer	$t=6.4$, $w=0.5$	Rubin *et al.*[g]
CB/polymer	$w=0.77$	Breeze *et al.*[h]
CB, graphite,…/talc wax	$w=1.28-1.36$ far from p_c	Chiteme and McLachlan[i]
	$w=0.36-1.1$ close to p_c	

[a]Reference 33.
[b]Reference 34.
[c]Reference 35.
[d]Reference 37.
[e]See Ref. 36.
[f]Reference 38.
[g]Reference 32.
[h]Reference 40.
[i]Reference 39.

Computation of exponents was done also[28] for the archetype of continuous percolation—namely, the random void (RV) model and its inverted version (IRV) (Table I). In the 2D (3D) RV model,[30] the resistors are the channels left between the circular (spherical) voids randomly made in the initial continuous surface (volume). The resistance is determined by the width of the channel, whose distribution is a diverging power law. Consequently, as already known for the t exponent of resistivity, a correction to κ and w is added with respect to the corresponding lattice values.

Modification of exponents is a specific feature of physical properties. Except conduction, it is also valid for fluid permeability or elastic constants.[30] Geometrical properties, like correlation length, are still described by the lattice values.

The computation of macroscopic resistance R involves evaluation of the average value $\langle R\rangle_L$ for a string of L singly connected bonds, which is dominated by the most resistive one. The nature of the probability distribution of bond resistance is thus determining in this computation. The assumption made in Ref. 30 is that, as the diameter ϵ of the channels approaches 0, its probability density has a finite limit. The exponents of Table I are derived from the relationship between resistance and channel diameter ($r\propto\epsilon^{-3/2}$ for RV in 3D, for instance).

Observation of large deviations of t, κ, and w values from theoretical prediction (in general experimental values are much larger; see Sec. VI B) has led Balberg[15] to revisit those models, removing the assumption of a uniform distribution of ϵ as $\epsilon\rightarrow 0^+$. Instead, the distribution is supposed to favor the smaller ϵ: for instance (and tractability), $P(\epsilon)\propto\epsilon^{-\omega}$ with $0<\omega<1$. Here $\langle r\rangle$ and $\langle\delta r^2\rangle$ are also power laws of ϵ, so that an analytical form for nonuniversal exponents t and κ can be derived.[15] The bounds for extended 2D and 3D RV and IRV models are given in Table I.

Among experimental systems that exhibit nonuniversal exponents are "touching-particles" ones, *a priori* relevant to ideal 3D IRV. Anomalous t is not expected in this case (Table I), because of the probability distribution of resistance of the narrowest channels (intersections of particles). However, considering tunneling percolation (TP) in a random arrangement of particles, the elementary resistances write as $r\propto\exp(l/\chi)$ (l is the distance between particles and χ the typical tunneling length). The $\{r\}$ distribution has the convenient power law decay, due to the exponential decrease of interparticle distance probability at large l. If the average distance is $\langle l\rangle=\lambda$, the additive correction to t is $\lambda/\chi-1$ (Ref. 31). Resistance fluctuations are estimated within the same approximation.[32] It is found that $\langle\delta R^2\rangle_L\propto L^{2\lambda/\chi-1}$ and thus $\langle\delta R^2\rangle_L/\langle R\rangle_L^2\propto L^1$ because $\langle R\rangle_L\propto L^{\lambda/\chi-1}$. Consequently κ is $\kappa_{\text{latt}}+1$ and w is written as shown in Table I.

B. Experimental exponents

In the previous paragraph, the wide dispersion of experimental results has already been quoted. We want to discuss some aspects of this fact, focusing on 3D composite systems, which resemble our blends. A significant part of the published results is collected in Table II. The conductive loading is often carbon black (CB).

Due to our own observations about the influence of experimental conditions on the noise amplitude, we will pay particular attention to the methods used. In any case, the voltage probes are at the surface of the material and cross the main current lines. The configurations are of the "rectangu-

lar" type, not of π type. To our knowledge, the only use of a nonconventional design was that already mentioned about electropolymerized conducting polymers.[22] Many samples are made of pressed pellets (flat cylinders) of compacted powders. In this case some of them are measured in the two-probe configuration,[35,37,39] the other in the four-probe configuration.[34] Electrical contacts are often made by a conducting paste,[32,34,37,39,40] a solution nonconvenient for conducting polymers due to the solvent of the paste, and otherwise by pressure of metallic electrodes.[33,35]

The first report of a clear scaling of S_V according to Eqs. (1) and (4) concerns a mixture of submicrometric carbon particles (CB) with wax.[33] Noise measurement is done by the four-probe method with pressed indium wires. The divergence at $p_c=10.8\%$ is much stronger ($\kappa=4$) than that predicted by the almost contemporaneous percolation theory ($\kappa=2.56$). Very close to p_c, for samples with resistance higher than 1 MΩ, bursts are observed in the temporal signal (popcorn noise). They are attributed to irreversible breaking of links and can be related to the deviation for the quadratic dependance of noise versus bias in this concentration region. Similar observations are reported on a 2D mixing of copper particules in polymer, accompanied by light flashes.[41] We never observed such an effect.

Comparable results ($w=1.7$) were obtained later by Nandi *et al.*[35] who also studied nonlinearity in S_V vs V^2 at high bias voltage. In the Ohmic regime, the exponents are very close to the previous ones (Table II), despite a difference in CB structure[36] (leading to $p_c=0.76\%$) and measurement procedure (pressed circular brass electrodes in two-probe configuration). At higher V, above an onset value where R begins to decrease, S_V has a weaker dependance on V and R. In that case it is found $w\simeq 0.5$.

The same $w=1.72$ is obtained in graphite/boron nitride compressed disks[37] when the measurement direction is perpendicular to the disk axis. A lower value $w=1.47$ is observed in the other direction. t exponents also exhibit anisotropy but to a lower extent and are moreover greater than t_{latt}^{3D}. This is tentatively attributed to a larger (divergent) distribution of local conductances, since t values are explained by the continuous percolation. The κ exponent is not directly determined in this paper.

In Ref. 34, the conductive fraction is definitely of metallic type: Ag-10 at % Pt alloy. The resistance of blends in tetrafluoroethylene above percolation threshold (21%) is a slowly decreasing function of temperature between 4 and 300 K. The PSD depends on frequency as $f^{-1.3}$. The normalized noise amplitude $fS_V(f)/V^2$ at 10 Hz is studied as a function of R. In the concentration range 23%–29%, two scaling regimes are observed: $w\simeq 1$ far from p_c, $w\simeq 3$ close to p_c. In the low-resistance regime, the authors claim that w is compatible with 3D lattice percolation $w=0.78$, and they invoke the IRV model for the high-resistance regime. $w=3$ is indeed the upper bound determined by Balberg[15] for the 3D extended IRV model, corresponding to the most diverging distribution of local resistances. The values are not compatible with the effective-medium approximation of Pierre *et al.*[41] (see below) in the case of good metallic contacts. It seems difficult to conciliate all the observations.

Two other recent publications[32,40] deal with CB/polymer mixing. In the first one,[32] "extreme" values are found for transport exponents: highest $t=6.4$, lowest $w=0.5$. None of the extensions of continuous percolation models are able to explain the low w value. Considering the low structure of CB—i.e., the fact that CB units are almost compact and nonaggregated spheres—the authors justify the use of the tunneling percolation model[31] that assumes a Hertz distribution for the distances between adjacent particles. This microstructure leads to a large value of the critical volume fraction: 39%. Nevertheless, the transport exponents of this mixing lead the authors to conclude that a "touching particle" model (like IRV) is irrelevant and consequently that the percolation is only electrical (tunneling), not geometrical. These results strongly contrast with those discussed in Ref. 40. In the latter, a fuse effect (differential dilation of CB and polymer with raising T) is use to drive continuously the samples through a metal-insulator transition. Whatever the CB content (17.5%–35%) above threshold (17.0%) a crossover temperature is found between a classical lattice percolation regime ($w=0.77$) and a quantum tunneling regime, at lower T and R, which is no longer described by a power law. The scaling due to quantum effects is $\ln S_\rho/\rho^2 \propto -1/\rho$, be it percolation or localization. In addition to these two regimes, observed on the metallic side of the transition, a nonpercolative one is found in the insulating side (for the sample with 35% CB) and $S_\rho \propto \rho^2$. Although the "universal" crossover seems well ascribed (see Fig. 3 of Ref. 40), the scalings are only defined in a tiny range: 1/3 of a decade. This is at variance to standard measurements for actual concentration changes, where, on average, the range covers three decades.

The most recent and extended work[39] also deals with CB (and other conductors) in talc wax. Measurements are made in two-probe configuration. As in our case, κ and w are independently extracted from data. The analyses developed in this paper are puzzling because eight κ's and w's exponents are given for each blend. The authors distinguish two regimes, close to (index 1) and further (index 2) from p_c (1.2%–3.5% depending on the conductive load), as already observed by Rudman *et al.*[34] κ_1 and κ_2 may differ abruptly, without a general rule concerning their ratio: 5.2 and 3.3 for raw CB, 0.9 and 2.6 for graphite. Nevertheless, it is always found that $w_1 < w_2$, which is the opposite of Ref. 34. Whereas κ's are defined as usual from S_V/V^2 scaling, the exponents $\kappa^{(m)}$ are also extracted from S_V/V^m scaling ($m \neq 2$) because the quadratic dependance on bias voltage is not always verified ($1 \leqslant m \leqslant 2$). No meaning is suggested for the interpretation of $\kappa^{(m)}$. The other four κ's are obtained for samples of reduced volume (ratio 1:13.5). They also dramatically differ from those for bigger samples and may be smaller or larger. This is contradictory with the basics of noise resistance and not discussed. At variance from noise scaling, resistance has a more standard behavior and a single t is found for each blend. As a consequence the consistency of scalings ($w=\kappa/t$) is lost. One should also point out that κ (w) exponents are define over narrow ranges: 0.5–1 (1–2) decade in S_V vs $p-p_c$ (R).

In the work by Pierre *et al.*[41] the scaling relation between S_V and R is assumed to be representative of the local mecha-

nisms responsible for the noise. The composites of copper particles in polymer are assumed to have a conductive fraction in the proximity of the percolation threshold, leading to a wide range of resistance and noise values. The data are not analyzed as a function of a concentration variable, but an effective medium approximation involving two systems characterized by $\{R_i, S_i\}_{i=1,2}$ is developed to account for the change between two regimes defined by $w=1.5$ and $w=1.0$ at low and high values of resistance, respectively. The first case corresponds to a Sharvin-type metallic junction (ballistic regime) between copper particles. The second case describes a noisy contact limited by a dirty oxide layer.

A specific effect of our all-polymer mixture is the stability of relative geometry of both phases with respect to temperature, resulting in a constant value of percolation threshold as T is varied. This contrasts with CB/polymer systems where the relative volumic fraction evolves with T. That is why, in our case, a variable T noise measurement would deserve attention. The change of local conductance distribution with T should also be reflected in a change in w and κ.

To our knowledge, there are no investigations of the thermal dependence of noise exponents in conventional percolating systems. However, scaling laws are also found in the transport properties of inorganic doped semiconductors as a function of carrier density. In a very recent paper,[42] the noise of a 2D hole system in a GaAs quantum well was investigated. Equation (4) is remarkably obeyed whatever the carrier density p_s (1.5 to 1.78×10^{10} cm^{-2} and the temperature (35–700 mK) with a single $w=2.4$. This is close to $w=2.6$ found in the 2D disordered lattice model.[29] It thus suggests a percolation phenomena, but the scaling variable is $x=p_s^2$. With this assumption, based on the interactions of carriers, the scaling $\ln\rho\propto(x-x_c)^{-t}$ is verified with t almost independent of T.

C. Conclusion

The review of experimental studies in 3D percolating systems reveals a wide dispersion of results and interpretations. Due to the absence of similar works on $1/f$ noise in conducting polymer blends, we cannot directly compare our findings to previous ones. Based on w exponent values, the closest ones seem to be high structure CB/polymer mixings.[38,39] This is not unexpected, in the sense that "high structure" implies a more ramified network as compared to "low structure," a synonym to globular arrangement.

To sum up, $1/f$ noise investigations in PANI(CSA)/PMMA blends confirm the heterogeneous disordered nature of the mixings. They moreover reveal that several kinds of inhomogeneities may be present, in a much more sensible way than other transport measurements do. Beside the ramified nature of the conducting network, already probed by the resistivity measurements as well as microstructural observations, it has been shown that the film surfaces are electrically different from the bulk and one from another, and that noisy isolated defects may conceal the bulk behavior, even if resistivity is not altered. Once these effects recognized and considered, the percolation scaling is well established on the entire explored range of PANI contents above percolation threshold and the consistency between transport percolation exponents t, κ, and w experimentally checked. Numerical values confirm that these blends pertain to the extended random void class of percolating sytems.

ACKNOWLEDGMENT

We thank C. Lombard for his crucial contribution to the instrumental development and the measurement protocol.

*Electronic address: jplanes@cea.fr

[1] Y. Cao, P. Smith, and A. J. Heeger, Synth. Met. **48**, 91 (1992).
[2] M. Reghu, C. O. Yoon, C. Y. Yang, D. Moses, P. Smith, A. J. Heeger, and Y. Cao, Phys. Rev. B **50**, 13 931 (1994).
[3] J. Planès, A. Wolter, Y. Cheguettine, A. Proń, F. Genoud, and M. Nechtschein, Phys. Rev. B **58**, 7774 (1998).
[4] C. Y. Yang, Y. Cao, Paul Smith, and A. J. Heeger, Synth. Met. **53**, 293 (1993); C. Y. Yang, M. Reghu, A. J. Heeger, and Y. Cao, *ibid.* **79**, 27 (1996).
[5] J. Planès, Y. Samson, and Y. Cheguettine, Appl. Phys. Lett. **75**, 1395 (1999); J. Planès, F. Houzé, P. Chrétien, and O. Schneegans, *ibid.* **79**, 2993 (2001).
[6] J. Fraysse, J. Planès, A. Dufresne, and A. Guermache, Macromolecules **34**, 8143 (2001).
[7] J.-P. Travers *et al.*, Synth. Met. **101**, 359 (1999); D. Djurado, J. Combet, M. Bée, P. Rannou, B. Dufour, A. Proń, and J.-P. Travers, Phys. Rev. B **65**, 184202 (2002).
[8] N. F. Mott and E. A. Davis, *Electronic Processes in Noncrystalline Materials* (Clarendon Press, Oxford, 1979).
[9] O. Quadrat, J. Stejskal, C. Klason, J. Kubat, and D. H. McQueen, J. Phys.: Condens. Matter **7**, 3287 (1995).
[10] J. Fraysse and J. Planès, Phys. Status Solidi B **218**, 273 (2000).
[11] J. Planès, S. Bord, and J. Fraysse, Phys. Status Solidi B **230**, 289 (2002).
[12] F. N. Hooge, Phys. Lett. **29A**, 139 (1969).
[13] For conducting polymers, the carrier density is not readily known as it can be for inorganic semiconductors doped with fully ionized shallow impurities. In our case, it is fixed by the chemical doping of PANI in solution, prior to mixing. Modification of the number N_c is obtained by a volume change.
[14] D. Stauffer, *Introduction to Percolation Theory* (Taylor & Francis, London, 1985).
[15] I. Balberg, Phys. Rev. B **57**, 13 351 (1998).
[16] P. M. Kogut and J. P. Straley, J. Phys. C **12**, 2151 (1979).
[17] A. Proń, Y. Nicolau, F. Genoud, and M. Nechtschein, J. Appl. Polym. Sci. **63**, 971 (1997).
[18] C. Ciofi, R. Giannetti, V. Dattilo, and B. Neri, IEEE Trans. Instrum. Meas. **47**, 78 (1998).
[19] A. François, Ph.D. thesis, Université Joseph Fourier, Grenoble, 2003, http://tel.ccsd.cnrs.fr/documents/archives0/00/00/53/42/index_fr. html
[20] B. Wessling, Synth. Met. **41**, 907 (1991).

[21] B. Wessling, in *Handbook of Nanostructured Materials and Nanotechnology*, edited by H. S. Nalwa, (Academic Press, San Diego, 2000), Vol. 5, p. 501.
[22] P. Bruschi and A. Nannini, J. Appl. Phys. **80**, 2279 (1996); P. Bruschi, A. Nannini, G. Serra, and E. Stussi, Thin Solid Films **289**, 242 (1996); P. Bruschi, A. Nannini, D. Navarrini, and M. Piotto, Fluct. Noise Lett. **2**, R1 (2002).
[23] L. K. J. Vandamme and G. Trefan, IEE Proc.-G: Circuits, Devices Syst. **149**, 3 (2002).
[24] L. K. J. Vandamme and P. P. Tijburg, J. Appl. Phys. **47**, 2056 (1976).
[25] E. P. Vandamme and L. K. J. Vandamme, Microelectron. Reliab. **40**, 1847 (2000).
[26] L. K. J. Vandamme, IEEE Trans. Electron Devices **41**, 2176 (1994).
[27] R. Rammal, C. Tannous, P. Breton, and A.-M. S. Tremblay, Phys. Rev. Lett. **54**, 1718 (1985).
[28] A.-M. S. Tremblay, S. Feng, and P. Breton, Phys. Rev. B **33**, 2077 (1986).
[29] C. Pennetta, G. Trefan, and L. Reggiani, Phys. Rev. Lett. **85**, 5238 (2000).
[30] B. I. Halperin, S. Feng, and P. N. Sen, Phys. Rev. Lett. **54**, 2391 (1985).
[31] I. Balberg, Phys. Rev. Lett. **59**, 1305 (1987).
[32] Z. Rubin, S. A. Sunshine, M. B. Heaney, I. Bloom, and I. Balberg, Phys. Rev. B **59**, 12 196 (1999).
[33] C. C. Chen and Y. C. Chou, Phys. Rev. Lett. **54**, 2529 (1985).
[34] D. A. Rudman, J. J. Calabrese, and J. C. Garland, Phys. Rev. B **33**, 1456 (1986).
[35] U. N. Nandi, C. D. Mukherjee, and K. K. Bardhan, Phys. Rev. B **54**, 12 903 (1996).
[36] A "low-structure" CB is made of particles whose shape is close to compact spheres and which are as isolated as possible from each other. A "high-structure" CB is made of hollow spheres (or spherical caps) aggregated in ramified clusters. The quantitative measurement relative to "structure" is adsorption of dibutylphtalate oil (Ref. 32).
[37] J. Wu and D. S. McLachlan, Phys. Rev. B **56**, 1236 (1997).
[38] A. Dziedzic and A. Kolek, J. Phys. D **31**, 2091 (1998).
[39] C. Chiteme, D. S. McLachlan, and I. Balberg, Phys. Rev. B **67**, 024207 (2003).
[40] A. J. Breeze, S. A. Carter, G. B. Alers, and M. B. Heaney, Appl. Phys. Lett. **76**, 592 (2000).
[41] C. Pierre, R. Deltour, J. VanBentum, J. A. A. J. Perenboom, and R. Rammal, Phys. Rev. B **42**, 3386 (1990).
[42] R. Leturcq, D. L'Hôte, R. Tourbot, C. J. Mellor, and M. Henini, Phys. Rev. Lett. **90**, 076402 (2003).